Evolutive Optical Fibers Combining Oxide and Chalcogenide Glasses with Submicronic Polymer Structures

Clément Strutynski, Moise Deroh, Rémi Bizot, Marianne Evrard, Frédéric Désévédavy, Grégory Gadret, Jean-Charles Jules, Claire-Hélène Brachais, Bertrand Kibler, Frédéric Smektala

Evolutive optical fibers combining oxide and chalcogenide glasses with submicronic polymer structures

Clément Strutynski, Moise Deroh, Rémi Bizot, Marianne Evrard, Frédéric Désévédavy, Grégory Gadret, Jean-Charles Jules, Claire-Hélène Brachais, Bertrand Kibler and Frédéric Smektala.*

Dr. C. Strutynski, Dr. M. Deroh, R. Bizot, M. Evrard, Dr. F. Désévédavy, Dr. G. Gadret, Dr. J.-C. Jules, Dr. C.-H. Brachais, Dr. B. Kibler and Prof. F. Smektala
Laboratoire Interdisciplinaire Carnot de Bourgogne (ICB)
UMR CNRS 6303, Université de Bourgogne Franche-Comté
21078 Dijon – France
Email: clement.strutynski@u-bourgogne.fr

Keywords: glass, polymer, optical fiber, multimaterial fibers, exposed-core fiber

Abstract

Multimaterial optical fibers combining tellurite with chalcogenide glasses and featuring thin polymer structures are fabricated via the thermal drawing process. We demonstrate that micrometric polyether sulfone films can be embedded within larger elongated tellurite/chalcogenide glass architectures. Taking advantage of the strong chemical reactivity contrasts which exist in the considered fiber geometries, a quasi-exposed-core waveguide is obtained by selective etching of the glass cladding. The potential of the post-processed fiber structure is then assessed through evanescent-wave probing of liquids and numerical investigations are carried out to establish the device performances as function of selected opto-geometric parameters. Those results open the way for the development of evolutive photonic objects benefiting from post-drawing processing of multimaterial fibers.

1. Introduction

In recent years, multimaterial fibers have enabled the development of a large number of novel photonic devices with tremendous innovative potential in numerous domains, such as biphotonic, environmental science, optoelectronics, remote sensing, medicine and so on.[1–5] The elaboration of such small-scale objects relies on the ability to combine through the thermal drawing process several materials (glasses, metals, polymers, semi-conductors, etc.) and, by extension, several functionalities within the same elongated structure.[6–8] From a fabrication standpoint, new materials associations are always sought to produce ever more original fiber architectures, thus solving modern technological challenges.[9–11] Glass/polymer combinations offer for instance great opportunities for the design and fabrication of functional optical fibers. In particular, the elaboration of fibers in which organic and inorganic materials are shaped together at the micro- or even at the nanometer scale provides promising prospects for infrared light-transmission, sensing, energy harvesting and others.[12,13] Another strong advantage of the combination of those diverse materials is the creation of highly heterogenous fiber geometries composed of domains with significant physicochemical property disparities. Thermoplastics and inorganic amorphous materials have for instance very specific chemical reactivities towards solvents or acids, and different processes such as redox reactions, dissolutions, etching, spatial segregation and so on, could be selectively triggered in fibered structures possessing strong compositional contrasts. Glass-polymer assemblies appear therefore useful for the implementation of simple and targeted post-processing procedures that would provide additional purpose to the fibers.

To this end, we here demonstrate the development of evolutive glass fibers integrating thin polymer structures. First, a simple multimaterial sandwich-like architecture is produced to assess the fiber-drawing ability of the proposed polymer/oxide glass preform profiles. Our approach appears original, especially when only few works in literature report on the association of thermoplastics with non-chalcogenide glasses for fiber development.[14] It is

found that large surface area polymer films with micrometric thickness can be successfully embedded within larger oxide-glass structures through the thermal drawing process and without compromising the organic material physicochemical integrity. This enables the production of elongated geometries in which specific domains are delimited by a polymer inclusion, which greatly simplifies post-drawing functionalization procedures. As a next step, a more sophisticated and functional fiber architecture which integrates a waveguiding core is considered. The fiber profile consists in a regular cylindrical core/cladding structure, except that the central chalcogenide core is wrapped within a thin polyether sulfone (PES) film with sub-micron thickness and embedded in a tellurite clad. Selective etching of the cladding is performed to produce quasi-exposed-core fibers. The purpose of the polymer is then twofold: (i) it preserves the chalcogenide glass core from the hydrochloric acid treatment carried out to remove the oxide glass cladding, and (ii) it provides mechanical protection for the etched portion of the fiber. The resulting fiber device is then tested in a proof-of-principle sensing experiment based on evanescent wave spectroscopy of liquids. Numerical investigations of modal properties are also carried out to further optimize the proposed fiber geometry and improve its sensing performances through interactions between the evanescent field and an analyte. We believe that small footprint optical detection systems could benefit from the use of such unique and evolutive photonic objects.

2. Materials selection

The different materials considered are listed in **Table 1**. A heavy oxide glass of composition (in mol. %) 60 TeO_2 – 20 ZnO – 20 Na_2O (TZN) is selected as cladding material, while a chalcogenide $Ge_{15}Sb_{20}S_{65}$ glass (GeSbS) with higher refractive index is selected as core material. Both glasses possess comparable glass transition temperatures (respectively 260 °C and 250 °C) and do not exhibit any crystallization event below 400 °C. This attests for their good thermal stability, which is essential for thermal drawing. Additionally, a polymer material,

namely polyether-sulfone (PES), is considered here because of its relatively high T_g of ~ 225 °C, which is one of the highest among amorphous polymers suitable for fiber drawing and makes it appropriate for co-drawing with the selected glasses. The glass transition temperature T_g, as well as the crystallization temperature T_x and the drawing temperature range T_{draw} of the different materials involved in the composite fibered structures are given in Table 1. [13,15–18]

Table 1. Properties of the materials considered in the present work.

Name	Composition	T_g	T_x	T_{draw}	$n_{@1.55\mu m}$
	Thin polymer film embedded in a glass fiber structure				
PES	$[OC_6H_4OC_6H_4SO_2C_6H_4]_n$	225 °C	-	275-325	1.621
TZN	60 TeO_2 – 20 ZnO – 20 Na_2O	260 °C	> 400 °C	315-375	1.838
	Quasi-exposed-core fiber				
PES	$[OC_6H_4OC_6H_4SO_2C_6H_4]_n$	225 °C	-	275-325	1.621
TZN	60 TeO_2 – 20 ZnO – 20 Na_2O	260 °C	> 400 °C	315-365	1.838
GeSbS	$Ge_{15}Sb_{20}S_{65}$	250 °C	> 400 °C	305-355	2.379

3. Thin polymer film embedded within a glass fiber structure

As a first experiment, a glass/polymer elongated arrangement is fabricated by the preform-to-fiber drawing method, as depicted in **Figure 1**a. It consists of a thin polymer film embedded within a rectangular glass structure. First, glass and polymer parts are selected and shaped (cutting and polishing) adequately. A 0.1 x 10 x 75 mm PES film is placed between two 2.9 x 10 x 75 mm TZN glass plates to form the preform.

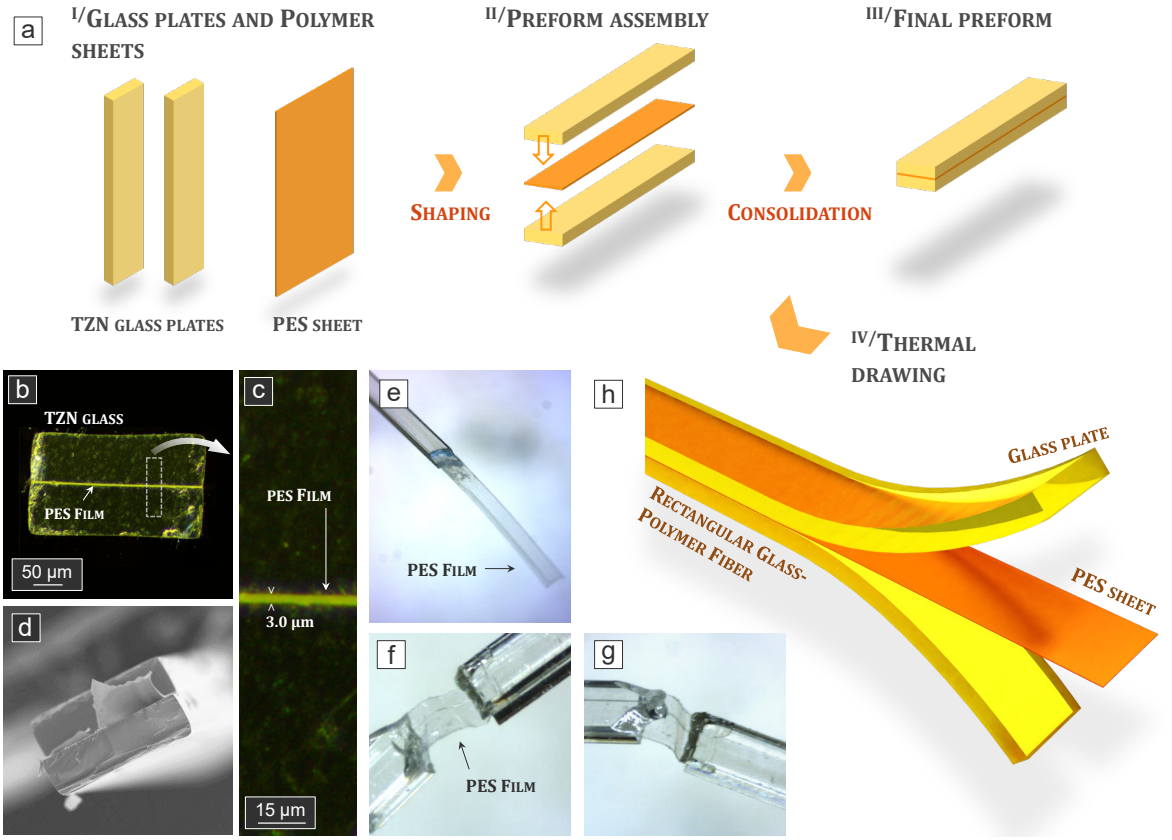

Figure 1. (a) Description of the fabrication process of the rectangular glass/polymer fiber: glass and polymer parts are shaped (cutting and polishing) adequately to form a macroscopic preform which is subsequently stretched down into meters of composite fiber. (b) Cross-sectional view of the glass/polymer fiber (175 x 300 µm). (c) View of the ~ 3.0 µm thick PES film at higher magnification. The micrographs were captured by means of an optical microscope in reflection mode. (d) SEM image (x 250) of a roughly cut TZN/PES fiber. (e) Image of a TZN/PES fiber dipped in HCl: the glass part is removed leaving only a thin polymer ribbon apparent at the extremity of the fiber. (f-g) Pictures of fractured segments of the composite fiber. (h) Diagram describing the glass-polymer structure.

The assembly is then consolidated at 280°C for one hour to ensure good adhesion between the different polymer and glass parts. A moderate pressure (few kPa) is applied on the stack by means of ceramic weights during this procedure. Following, the preform is thermally stretched down into meters-long composite fiber. Cross-sectional view of the fabricated structure is shown on Figure 1b. The rectangular TZN glass frame has outer dimensions of ~ 175 x 300 µm (see Figure 1b), while the PES sheet possesses a ~ 3.0 µm thickness (see Figure 1c). For the sake of clarity, a diagram describing the fabricated fiber is given on Figure 1h. A thin polymer inclusion has been successfully embedded within the TZN glass structure. Remarkably, the

organic film possesses a constant thickness across the whole fiber width (i.e., no significant deformation undergone during thermal drawing). Additionally, the initial preform profile is fully transferred to the fiber as the ratio between the polymer thickness and the glass external dimensions is preserved during the stretching operation. Glass to polymer thickness ratio is 5.9/0.1 = 59 on the preform and 175/3.0 = 58.3 on the fiber. Conservation of the initial profile is ensured by finely controlling the materials viscosity during thermal drawing of the preform which is elongated in a homothetic fashion.

Further compositional investigations were carried out through Energy-Dispersive X-ray (EDX) spectroscopy analysis. Sulfur is targeted for the mapping of zones related to polyether-sulfone inclusions while tellurium helps to identify regions which corresponds to the TZN glass. For clarity, spatial distributions of sodium, zinc and carbon are not presented here. The 2D distributions at the fiber cross-section of tellurium and sulfur are shown in **Figure 2**c and d, respectively. No contamination nor inter-diffusion potentially occurring at the vicinity of the glass/polymer interface could be evidenced from those measurements. Additionally, the distributions of Te and S atoms along a line perpendicular to the glass/polymer/glass structure are plotted in Figure 2e. The repartition of tellurium and sulfur is symmetrical with respect to the median plane of the polymer film. This confirms that no reaction occurs between the glass and the polymer during the temperature-based elongation of the preform. This original approach demonstrates the possibility to manufacture complex fiber architectures which involve for the first time low T_g oxide glasses and polymers. Glass/polymer associations are generally restricted to the combination of high-performance polymers (such as Polysulfones) with chalcogenide glasses, mainly due to thermal compatibility issues.[12,13] With few exceptions,[14] oxide-based glasses have either too high glass transitions temperatures or too poor thermal stability to be thermally stretched with organic materials.

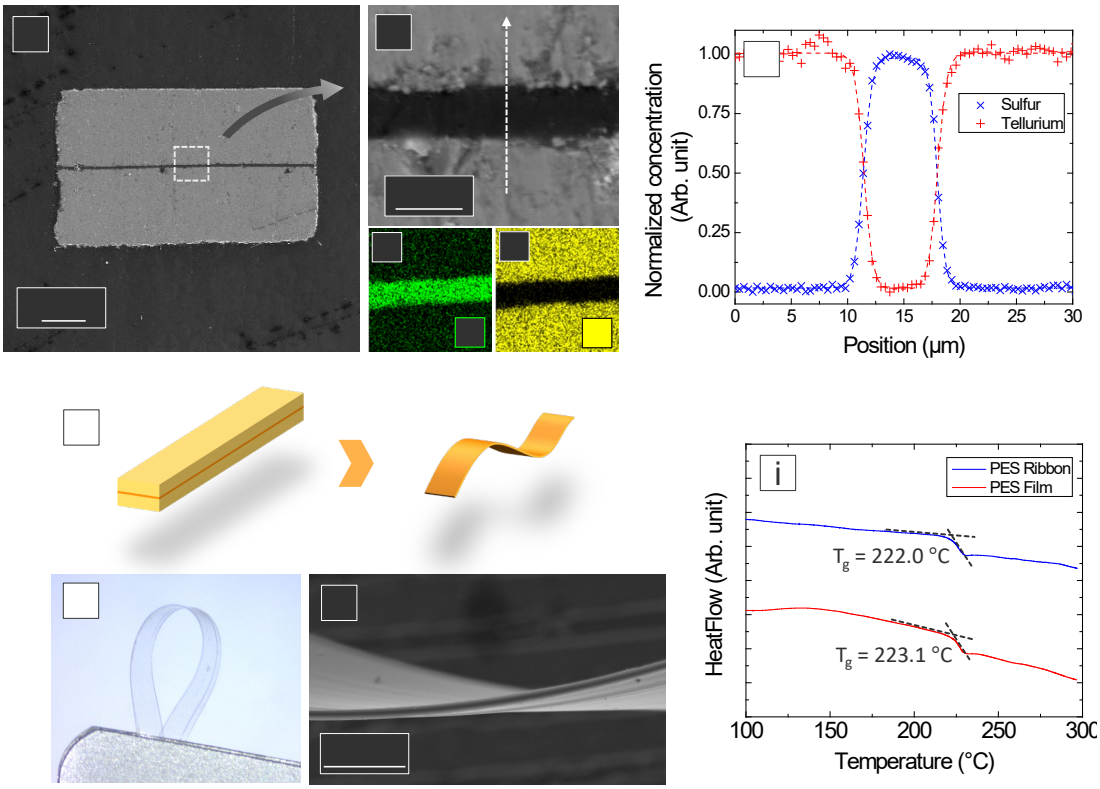

Figure 2. (a) SEM image (x 75) of the TZN/PES multimaterial fiber cross-section. The fiber dimensions are ~ 500 x 850 µm. (b) SEM image (x 1200) of the glass/polymer/glass structure. The polymer film is approximately 8 µm thick. (EDX spectroscopy analysis of (c) sulfur and (d) tellurium 2D-distributions at the vicinity of the polymer inclusion. (e) EDX distribution profile of tellurium and sulfur along a line perpendicular to the glass/polymer/glass structure. The investigated profile line is indicated with a white dashed arrow in subplot (b). (f) Description of how the PES ribbons are obtained from the composite fiber: fiber segments are immerged few minutes in concentrated hydrochloric acid (HCl ~ 6 mol L^{-1}) in order to remove the glass parts. The polymer ribbons are then thoroughly rinsed in clean deionized water to get rid of HCl. (g) Picture and (h) SEM image (x 550) of the obtained polymer ribbons. (i) DSC curves of the PES sheet prior and after the fiber drawing process.

As the TZN parts represent ~ 97 % of the volume of the composite preform considered here, its thermal stretching is performed at the glass drawing temperature (300-325 °C), which is approximately 25 °C higher than that of polyether-sulfone (see Table 1). To ensure that the polymer did not suffer any degradation during its stretching, post-drawing integrity of PES is assessed through Differential Scanning Calorimetry (DSC). DSC measurements are carried out on bare polymer ribbons which are obtained by immerging ~ 10 cm segments of the composite fiber in concentrated hydrochloric acid (HCl ~ 6 mol L^{-1}) for few minutes. This step helps to dissolve the glassy parts of the fiber, as shown on Figure 2f. The bare polymer samples are then thoroughly rinsed in clean deionized water to get rid of HCl and subsequently dried in a hoven

set at 120 °C for 30 minutes. Images at of the obtained polymer ribbons are provided in Figure 2g and h. DSC measurements are then carried out on those samples and compared to the initial PES film involved in the preform fabrication. The results are recapped in Figure 2i. Both DSC curves of PES, prior and after thermal drawing, exhibit an endothermic event around 222 °C (223.1 °C and 220.0 °C for the initial and the drawn PES film respectively) corresponding to their glass transition temperature. The comparative differential scanning calorimetry does not reveal any deviation of the polyether-sulfone glass transition temperature. Consequently, the polyether-sulfone sheet did not undergo any degradation during the fiber drawing and its physicochemical integrity is preserved.

4. Quasi-exposed-core fibers

4.1. Fiber design

A more sophisticated fiber architecture is now produced using a similar fabrication method as the one described in the previous section. The preform consists this time in two TZN half-cylinders (9 mm outer diameter) with a groove on their internal surface. The glass parts are processed so that the groove is parallel to the main axis of the half-cylinders. A 0.98 mm chalcogenide cylindrical glass cane wrapped within two 50 µm thick PES sheets is placed between those TZN parts. This means that the chalcogenide glass core is not in direct contact with the tellurite glass cladding. The stack is then annealed à 280 °C for one hour for consolidation purposes, as previously mentioned. Description of the different preform preparation steps is depicted in **Figure 3**a. The preform is then thermally elongated using a dedicated 3-m-high draw tower. Optical micrographs of the fabricated fibers are shown in Figure 3b.

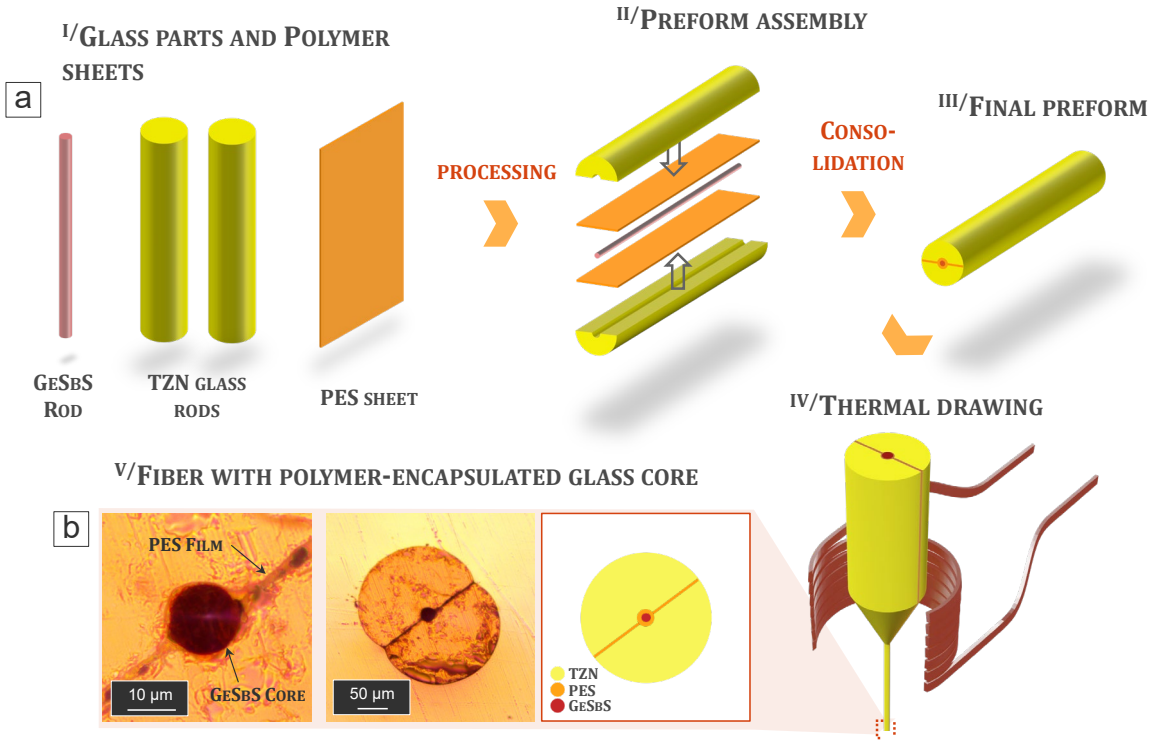

Figure 3. (a) Description of the fabrication process of multimaterial fibers with polymer-protected glass core: glass and polymer parts are shaped (cutting, mechanical drilling, polishing) adequately to form a macroscopic preform which is subsequently stretched down into meters of composite fiber. (b) 2D diagram describing the fiber cross section (right panel), cross-sectional view of the whole fiber (central panel) and its core (left panel). The images were captures using an optical microscope in transmission mode.

The overall initial profile is again well preserved throughout the thermal elongation process. The thin polymer structure completely encapsulates the core, keeping it isolated from the external oxide glass cladding. Slight variations of the PES film can however be observed. Again, further compositional investigations are carried out using EDX spectroscopy analysis. Here, carbon is targeted for the mapping of zones related to polyether-sulfone inclusions while tellurium and germanium help to identify regions which correspond to the TZN and GeSbS glasses, respectively. The 2D distributions at the fiber cross-section of germanium, tellurium and carbon are measured and shown in **Figure** 4c, d, and e, respectively.

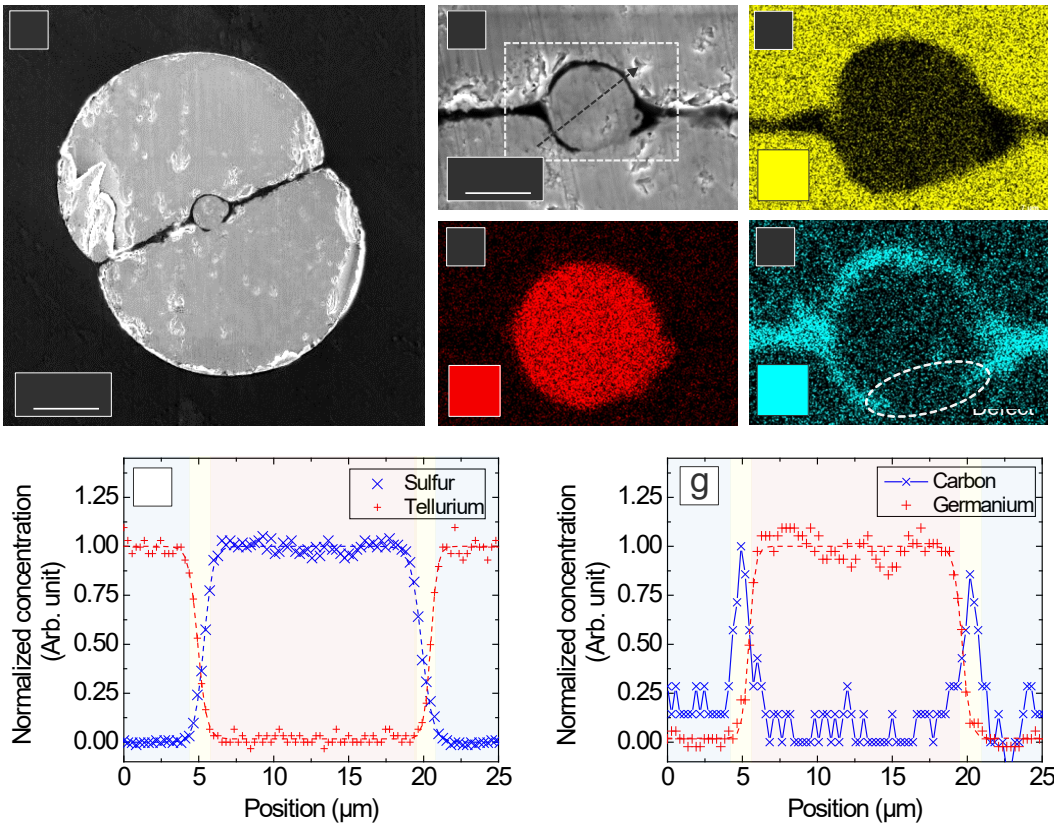

Figure 4. SEM images of (a) the multimaterial fiber cross-section (x 250) and (b) the chalcogenide glass core (x 2000). The diameter of the core is ~ 14.2 µm. 2D-distributions (c) Germanium, (d) Tellurium and (e) Carbon measured through energy-dispersive X-ray (EDX) spectroscopy analysis in the area indicated by the white dashed rectangle in subplot (b). EDX distribution profile of (f) tellurium and sulfur and (g) carbon and germanium along a line running across the core center (see black dashed arrow in subplot (b)).

Minor deformations of the structure are evidenced, especially in the bottom right part near the GeSbS core. A portion of the polymer film is missing (see Figure 4e), thus provoking a distortion of the core (see Figure 4c) as well as the cladding (see Figure 4d). It is worth noting that the different organic and inorganic compositional domains are well separated and no contamination nor inter-diffusion at the vicinity of the different glass/polymer interfaces are detected. EDX distribution profiles along a line running across the core center are given on Figure 4f and 4g for, respectively, tellurium and sulfur, and for carbon and germanium. The repartition of the different species is symmetrical with respect to the center of the germanium-rich core, which further confirms that the glass/polymer interfaces are not altered during the elongation process. Aside from where the two polyether-sulfone films recombine on each side

of the 14.2 µm GeSbS core, the thickness of the organic coating is approximately 0.7 µm and remains fairly unchanged around the chalcogenide glass. Conservation of the initial preform profile is confirmed, namely core diameter to PES film thickness ratios are 0.98 / 0.05 = 19.60 and 14.2 / 0.7 = 20.03 for the preform and the fiber, respectively.

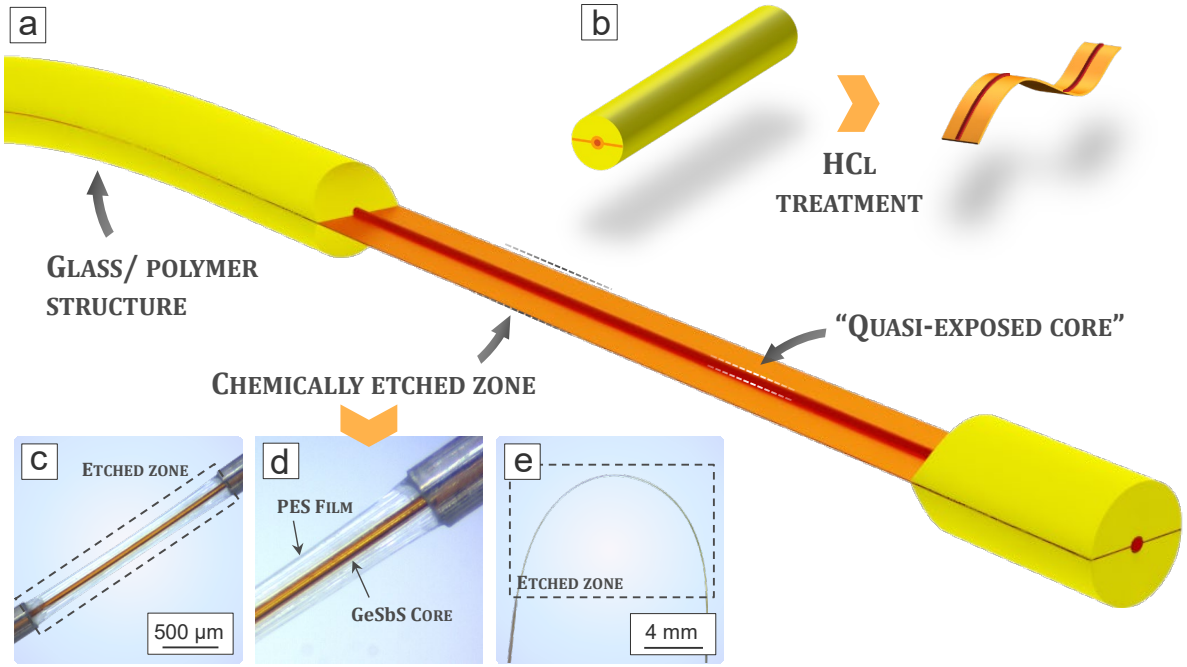

Figure 5. (a) 3D diagram of a core-cladding composite fiber with a portion of the structure stripped from its TZN glass cladding. (b) Description of how the quasi-exposed-core portions of the fiber are obtained from the initial composite structure: fiber segments are exposed few minutes to concentrated hydrochloric acid (HCl ~ 6 mol L^{-1}) on a ~ 2 to 6 cm zone in order to remove the TZN glass parts. The etched zone is then thoroughly rinsed with clean deionized water to get rid of any excess HCl. (c) and (d) longitudinal views of the chemically etched zone of the fiber. (e) Picture of a bent portion of the chemically etched fiber.

This unique combination of diverse materials within a single elongated structure offers interesting opportunities for the development of post-drawing evolutive fiber components. Here, by taking advantage of the strong chemical reactivity contrast which exists in the present composite fiber geometry, selective etching is performed to produce a quasi-exposed-core waveguide suitable for evanescent-wave probing of liquids. In literature, exposed core geometries are produced from step-index or microstructured fibers which are processed in particular manners. All solid architectures are generally side-polished to reduce the cladding thickness and expose the central core.[19] Air/glass microstructured fibers with exposed core are

prepared either from the drawing of specially prepared preforms (with one opened air channel[20]) or from various post-drawing processing methods of the as-drawn fibers (etching, micro-machining, etc.[21–24]). Here, the initial fiber is exposed to a solution of ~ 6 mol L^{-1} hydrochloric acid for few minutes as described in **Figure 5**b, which completely dissolves the oxide glass used as cladding material. Because of its good resistance towards HCl, the PES thin film remains intact after the acidic treatment and protects the chalcogenide glass core. A 3D diagram of the produced structure is shown in Figure 5a. Additionally, the polymer membrane provides mechanical strength to the etched part of the device, which helps to preserve the light-guiding core from breaking. Pictures of a stripped portion of the present fiber are shown in Figure 5c and d. The GeSbS core is stripped from its oxide glass cladding but is still wrapped within a thin polymer coating, i.e., a quasi-exposed core fiber. When the polymer film is thin enough, interactions can occur between the evanescent field of the guided mode from the fiber core and an analyte present at the vicinity of the etched part.

4.1. Evanescent wave probing of liquids

In this section, the potential of the above fiber device for evanescent-wave spectroscopy of liquids is assessed. More precisely, transmission of the quasi-exposed-core fiber is tested when the stripped portion is exposed to liquid deionized water. This detection configuration is similar to fiber evanescent wave spectroscopy (FEWS) sensors, which are based on the interactions between an analyte and the evanescent field of the guided mode from a straight or bent fiber or taper.[25–27] The experimental setup used for our proof-of-principle experiment is depicted in **Figure 6**a. A home-made fiber supercontinuum (SC) source is used as a wideband infrared light source for spectroscopic investigations. The SC is generated through nonlinear propagation of 70-fs pulses at 1560 nm, delivered by a compact fiber laser with nJ-level energy and 80 MHz repetition rate, in a single-mode GeO_2-doped silica fiber (HLNF). The SC source operates in the 1300 – 2100 nm range with an average output power of ~ 90 mW. The generated light is

then butt-coupled into the glass/polymer fiber using a precision translation stage while the output signal is collected using an InF_3 multimode fiber and sent to an Optical Spectrum Analyzer (OSA). It is worth mentioning that a polarization controller is inserted in the experimental setup to check for any polarization-dependent effects.

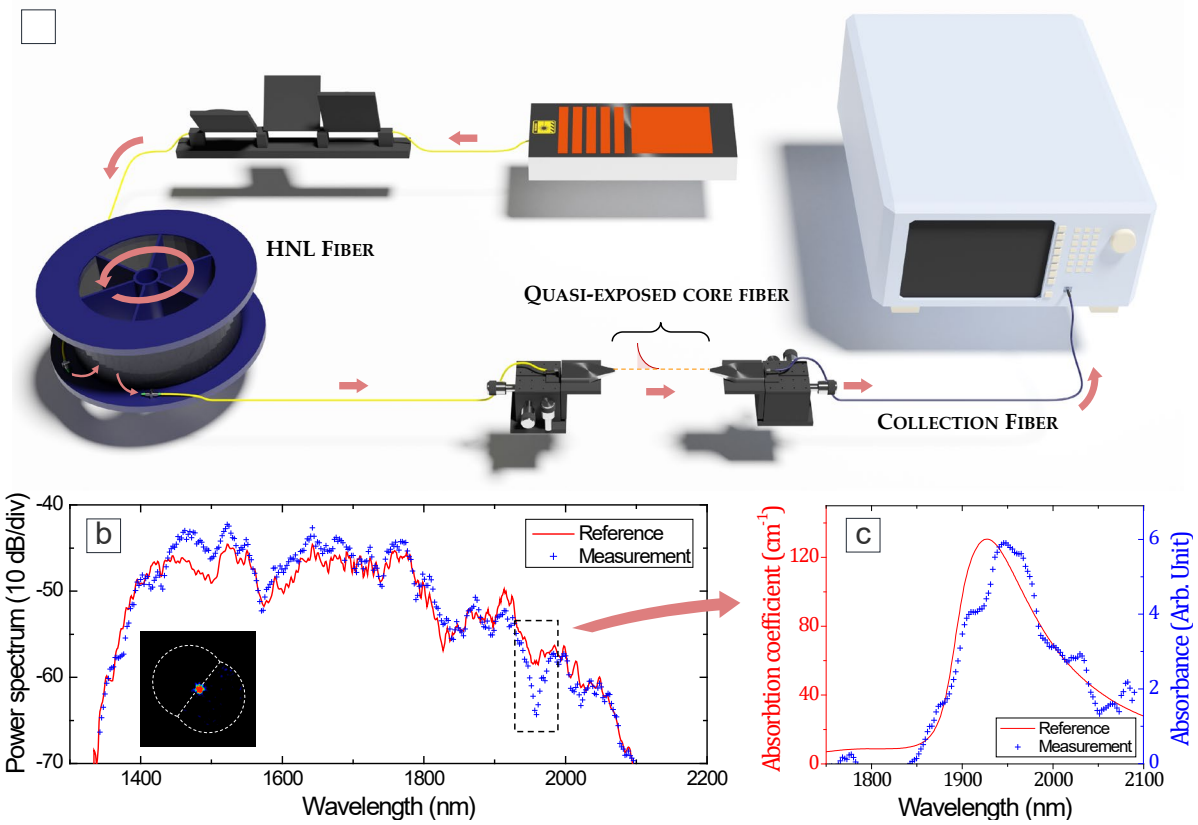

Figure 6. (a) 3D diagram of the setup used for the evanescent wave probing of liquids. (b) Transmission spectra of the quasi-exposed-core fiber in air (red line) and in deionized water (blue symbols). Inset: image of the output section of the fiber taken with an IR camera. (c) Comparison of the measured absorption spectrum (blue symbols) and the reference absorption spectrum of water (red line).[28]

In practice, evanescence-wave probing experiments are performed as follow: a reference spectrum is first recorded when the fiber is not exposed to any analyte. Then, the fiber is dipped in a liquid and a second spectrum is recorded. As a proof-of-principle experiment, measurement of liquid deionized water absorption is carried out using the above setup. The related reference and measurement spectra are plotted in Figure 6b (Red line and blue symbols respectively). A strong water-related absorption centered at ~1950 nm can be observed. The corresponding

absorption spectrum is shown in Figure 6c (blue symbols) and compared to literature (red line).[28] The measured and reference spectra both exhibit similar shape over the full spectral range, which validates the present system for optical probing of liquid samples.

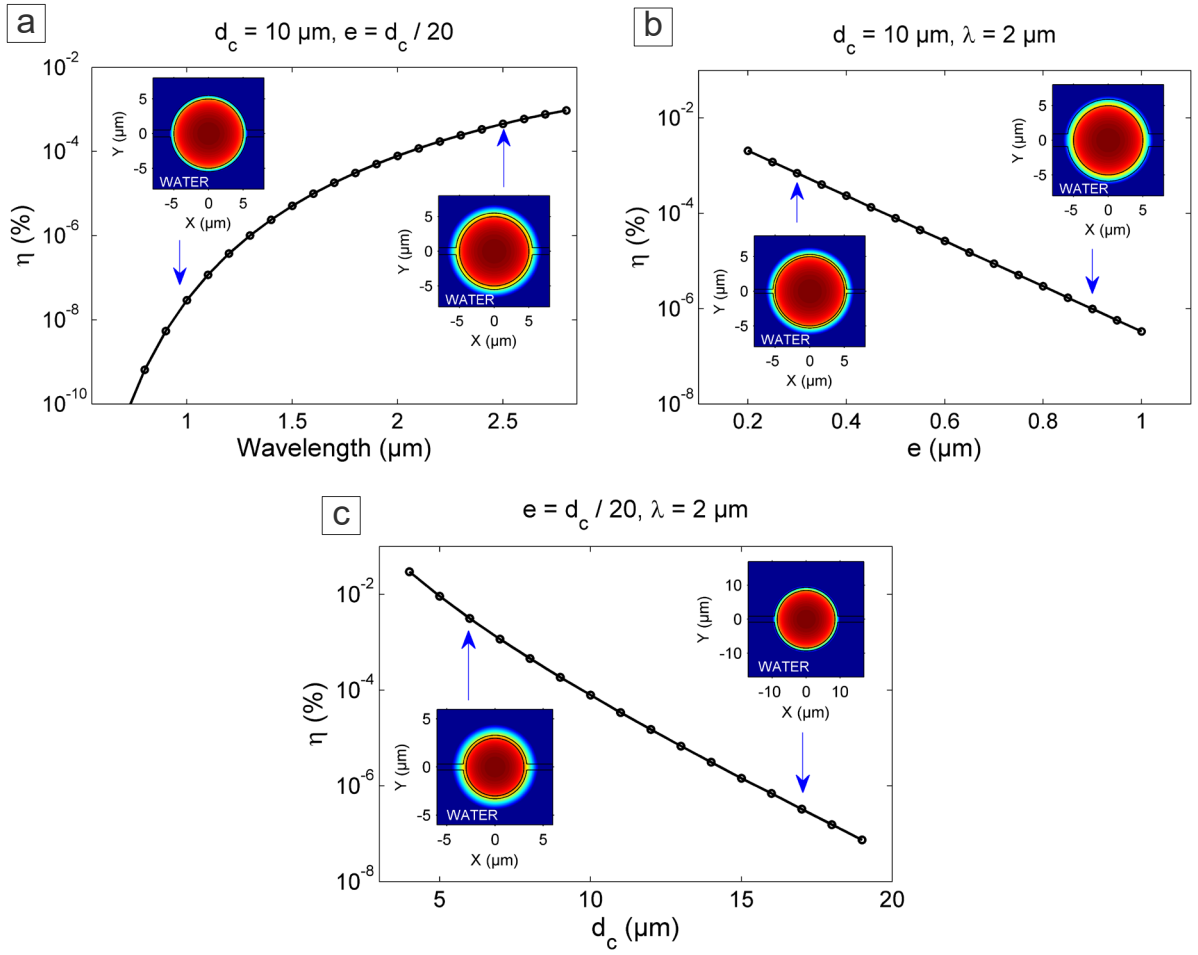

Figure 7. Numerical calculations of evanescent power fraction η (plotted in log. scale) inside the analyte as function of (a) wavelength, (b) polymer film thicknesses and (c) core diameter d_c. Insets: Intensity profiles for the fundamental propagation mode calculated for selected parameters.

Numerical investigations are then carried out to analyze the impact of the main physical parameters on the potential of our quasi-exposed-core fibers for evanescent wave probing of liquids. We considered an ideal cross-section of the quasi-exposed core encapsulated by the thin polymer film. Our detailed analysis of modal field and power distribution is only performed for the fundamental mode of our fiber device by means a commercial solver. Despite the multimode nature of the large-core waveguide, we checked that we coupled SC light into the

fundamental mode. It is worth mentioning that a multimode analysis could provide further insights into sensitivity enhancement or limitation of the fiber sensor.[29] In the present glass/polymer fiber architecture, sensitivity of the sensing device is directly related to the portion of evanescent field which interacts with the liquid analyte during light propagation in the quasi-exposed-core. The fraction of power outside the waveguiding structure (core + polymer thin film) $\boldsymbol{\eta}$, is calculated for the fundamental mode as function of different parameters, as shown in **Figure 7**. First, evolution of $\boldsymbol{\eta}$ as function of the wavelength is plotted in Figure 7a. As expected, the evanescent field extends further outside the core at longer wavelengths, for which the mode area is larger. In the meantime, the fraction of power outside the waveguiding structure decreases in a similar fashion when either the polymer film thickness or the core diameter increases, as depicted in Figure 7b and c respectively. Indeed, reducing the core size is the usual way to maximize the evanescent wave energy fraction (i.e., fiber tapering).[30]

In the case of the fiber used for the evanescent wave probing of deionized water, which has a core diameter d_c = 14.2 µm and a PES film thickness e = 0.7 µm, the portion of power probing the analyte is approximately 10^{-5} % at 2.0 µm, close to the considered water absorption band. Despite this low value, it was still possible to detect the absorption peak by propagating light through a ~ 7 cm long etched portion of the fiber. Further investigations are needed to fully grasp the potential of the proposed fiber geometry, and reach sensitivity and reusability of state-of-the-art sensors based on multi-material fibers.[31–33] The present numerical investigations provide interesting insight regarding this matter. Significant optimization of the device can be achieved by reducing the core diameter as well as the polymer thickness, as long as capillary break-up conditions are not met. For instance, a reduction of the dimensions of the fiber by a factor of two, i.e. producing waveguides with a ~7 µm core and a ~ 0.3 µm thick PES film (which is feasible via the thermal drawing process), would improve the evanescent power fraction by two orders of magnitudes. The ratio between the core diameter and polymer

thickness could also be changed on the initial preform to produce fibers with optimized geometry. The sensitivity could also be improved over several orders of magnitudes when operating the device at longer wavelengths, which is enabled by the considered materials (transmission up to 4.5 μm and 7 μm on respectively tellurite and GeSbS fibers).[17,34]

5. Conclusion

Multimaterial fiber geometries featuring thin polymer structures have been investigated in this work. The fabrication methodology relies on the simultaneous drawing of tellurite glasses together with thin polyether sulfone sheets around a chalcogenide glass core. The fiber profile is designed so that portion of the fibered structure can be processed into quasi-exposed-core waveguides through selective etching of the cladding glass. The device is then used in a proof-of-principle experiment which takes advantage of interactions between the evanescent field and a liquid analyte. Absorption spectroscopy measurement is carried out on deionized water from which the 1950 nm absorption band is detected. The efficiency of the exposed-core waveguide as function of wavelength, core diameter and polymer thickness is numerically investigated for future optimization of the fiber geometry. Our results confirm that the post-thermal-drawing processing of multimaterial fibers which possess high chemical reactivity contrast are promising for the development of all-in-one lab-on fiber solutions. Other glass/polymer associations could be considered for the development of similar structures, as long as the selected materials possess comparable drawing temperature ranges and distinct reactivities towards specific solvents. Hydrofluoric acid could be used to dissolve a silicate glass cladding or moisture sensitive phosphate glass parts could be removed with hot water.

Beside the improvement of the sensitivity of the system elaborated here, tailoring of the wave-guiding properties (dispersion, effective cross-sectional area, etc.) of the fiber could enable the monolithic implementation of a wideband MIR source based on supercontinuum generation. Given the optical assets of the selected materials (transmission window, nonlinear properties,

etc.),[35] the spectral broadening of femtosecond pulses would occur within the first few centimeters of the waveguide and the generated light would serve as the incident source.[36] Surface functionalization of the polymer in which the glass core is wrapped could also be looked at,[37] and would provide selectivity towards targeted compounds contained in body fluids, waste water or other liquid analytes of interest. Ultimately, extremely compact monolithic bio-sensors and innovative photonic devices could be produced from the assemblies proposed here.

6. Experimental Section

Glass synthesis: Oxide-based glass of composition (in mol. %) 60 TeO_2 – 20 ZnO – 20 Na_2O (TZN) is prepared using the standard melt-quenching technique. High purity precursors (99.99 %) are weighed in adequate ratios and are melted inside a platinum crucible placed in an electric furnace. Melting is carried out under room atmosphere for 30 min at 800 °C. The hot liquid is then poured into a brass mold preheated at 210 °C. The shape of the mold is chosen to produce either cylindrical (9 mm diameter and ~ 6 cm long) or parallelepipedal preforms (with dimensions of ~ 3 x 10 x 75 mm). Following, the glass is annealed at 250 °C for 5 hours to relieve any residual mechanical stress caused by the quenching. Finally, the temperature is gradually ramped down (2°C min^{-1}) to room temperature. Chalcogenide glass samples of composition $Ge_{15}Sb_{20}Se_{65}$ are prepared by the melt-quenching technique. High purity (99.999 %) elemental raw materials are weighed according to the desired stoichiometry and placed inside a silica setup previously cleaned using hydrofluoric acid (HF). The batch is then placed under secondary vacuum (10^{-8} bar) for 24 hours to remove any moisture adsorbed at the surface of the precursors or the silica recipient. The ampoule is then sealed and introduced in a rocking furnace and heated up to the refining temperature of 850 °C for 12 hours. After this, the molten batch is rapidly cooled down in a 25 °C water bath to obtain the glass. Finally, the glass is annealed at 240 °C for 5 hours after which the temperature is slowly ramped down (2°C min^{-1}) to room temperature.

Preform preparation and fiber drawing: The preforms are fabricated by stacking different glass and polymer parts which are manufactured through the following procedures. TZN glass parallelepipedic parts are straight forwardly obtained by carefully polishing rough glass pieces produced using a parallelepiped mold for the quenching. Grooved half-cylinders are manufactured from 9 mm diameter and 60 mm long cylindrical TZN glass rods in which a 1 mm diameter and 30 mm long hole is mechanically drilled at their center, forming a tube. After that, the tube is longitudinally polished to half its volume to produce a half cylinder with a central groove. ~ 1 mm. GeSbS glass canes are also used in the preform fabrication procedure. They are obtained from the thermal elongation of cylindrical GeSbS glass preforms with a diameter of 12 mm. Polyether-sulfone (PES) films of chosen dimensions are cut from an initial 50 µm thick sheet. The desired thickness of polymer in the preform is obtained by stacking the adequate number of the initial PES films (one layer for 50 µm, two layers for 100 µm, etc.). The adequate glass and polymer parts are selected depending on the targeted profile and the different elements are then stacked to form the preform. After that, a 2-hour consolidation treatment of the preform is performed at 280 °C. During this procedure a few kPa pressure is applied to the macroscopic arrangement by means of ceramic weights. Finally, the preform is placed inside the furnace of a draw tower of which the temperature is slowly ramped up (10°C min^{-1}). To avoid any contamination, a 3L min^{-1} He gas flow is applied during the procedure. After the initiation of the elongation process, the preform is slowly fed into the furnace while the drawing parameters are continuously monitored to produce the fiber with the desired dimensions.

Acknowledgements

Funding for this work has been provided from the French Government, managed by the French National Research Agency (ANR) through the French “Investissements d’Avenir” program, “4D Méta project” ISITE-BFC (contract ANR- 15-IDEX-0003), and by the European program

FEDER, the EUR EIPHI Graduate School (grant number ANR-17-EURE-0002) and the Conseil Régional de Bourgogne Franche-Comté through the "SMILE Project"

Received: ((will be filled in by the editorial staff))
Revised: ((will be filled in by the editorial staff))
Published online: ((will be filled in by the editorial staff))

References

[1] N. Myrén, H. Olsson, L. Norin, N. Sjödin, P. Helander, J. Svennebrink, W. Margulis, *Opt. Express* **2004**, *12*, 6093.

[2] A. L. Chin, S. Jiang, E. Jang, L. Niu, L. Li, X. Jia, R. Tong, *Nat. Commun.* **2021**, *12*, 5138.

[3] T. Zhang, K. Li, J. Zhang, M. Chen, Z. Wang, S. Ma, N. Zhang, L. Wei, *Nano Energy* **2017**, *41*, 35.

[4] Z. Wang, M. Chen, Y. Zheng, J. Zhang, Z. Wang, J. Yang, Q. Zhang, B. He, M. Qi, H. Zhang, K. Li, L. Wei, *Adv. Devices Instrum.* **2021**, *2021*, 1.

[5] G. Tao, A. M. Stolyarov, A. F. Abouraddy, *Int. J. Appl. Glas. Sci.* **2012**, *3*, 349.

[6] F. Sorin, A. F. Abouraddy, N. Orf, J. Shapira Oferand Viens, J. Arnold, J. D. Joannopoulos, Y. Fink, *Adv. Mater.* **2007**, *19*, 3872.

[7] S. Danto, F. Sorin, N. D. Orf, S. A. Wang Zhengand Speakman, J. D. Joannopoulos, Y. Fink, *Adv. Mater.* **2010**, *22*, 4162.

[8] W. Yan, C. Dong, Y. Xiang, S. Jiang, A. Leber, G. Loke, W. Xu, C. Hou, S. Zhou, M. Chen, R. Hu, P. P. Shum, L. Wei, X. Jia, F. Sorin, X. Tao, G. Tao, *Mater. Today* **2020**, *35*, 168.

[9] A. F. Abouraddy, M. Bayindir, G. Benoit, S. D. Hart, K. Kuriki, N. Orf, O. Shapira, F. Sorin, B. Temelkuran, Y. Fink, *Nat. Mater.* **2007**, *6*, 336.

[10] M. Alexander Schmidt, A. Argyros, F. Sorin, *Adv. Opt. Mater.* **2016**, *4*, 13.

[11] W. Yan, A. Page, T. Nguyen-Dang, Y. Qu, F. Sordo, L. Wei, F. Sorin, *Adv. Mater.* **2019**, *31*, 1802348.

[12] J. J. Kaufman, G. Tao, S. Shabahang, D. S. Deng, Y. Fink, A. F. Abouraddy, *Nano Lett.* **2011**, *11*, 4768.

[13] K. Kuriki, O. Shapira, S. D. Hart, G. Benoit, Y. Kuriki, J. F. Viens, M. Bayindir, J. D. Joannopoulos, Y. Fink, *Opt. Express* **2004**, *12*, 1510.

[14] M. Rioux, Y. Ledemi, S. Morency, E. S. de Lima Filho, Y. Messaddeq, *Sci. Rep.* **2017**, *7*, 43917.

[15] L. Brilland, J. Troles, P. Houizot, F. Désévédavy, Q. Coulombier, G. Renversez, T. Chartier, T. N. Nguyen, J.-L. Adam, N. Traynor, *J. Ceram. Soc. Japan* **2008**, *116*, 1024.

[16] G. Xu, W. Zhang, Y. Huang, J. Peng, *J. Light. Technol.* **2007**, *25*, 359.

[17] J. Troles, Y. Niu, C. Duverger-Arfuso, F. Smektala, L. Brilland, V. Nazabal, V. Moizan, F. Desevedavy, P. Houizot, *Mater. Res. Bull.* **2008**, *43*, 976.

[18] Y. Hu, K. Tian, T. Li, M. Zhang, H. Ren, S. Qi, A. Yang, X. Feng, Z. Yang, *Opt. Mater. Express* **2021**, *11*, 695.

[19] S.-M. Tseng, C.-L. Chen, *Appl. Opt.* **1992**, *31*, 3438.

[20] R. Kostecki, H. Ebendorff-Heidepriem, C. Davis, G. McAdam, S. C. Warren-Smith, T. M. Monro, *Opt. Mater. Express* **2012**, *2*, 1538.

[21] C. Martelli, P. Olivero, J. Canning, N. Groothoff, B. Gibson, S. Huntington, *Opt. Lett.* **2007**, *32*, 1575.

[22] A. van Brakel, C. Grivas, M. N. Petrovich, D. J. Richardson, *Opt. Express* **2007**, *15*, 8731.

[23] S. C. Warren-Smith, H. Ebendorff-Heidepriem, T. C. Foo, R. Moore, C. Davis, T. M. Monro, *Opt. Express* **2009**, *17*, 18533.

[24] R. Kasztelanic, A. Filipkowski, D. Pysz, R. Buczynski, *Opt. Express* **2018**, *26*, 32374.

[25] A. P. Velmuzhov, V. S. Shiryaev, M. V. Sukhanov, T. V. Kotereva, B. S. Stepanov, G. E. Snopatin, *J. Non. Cryst. Solids* **2022**, *579*, 121374.

[26] X. Wang, J. Su, Y. Wang, C. Yang, S. Dai, P. Zhang, *J. Non. Cryst. Solids* **2021**, *559*, 120686.

[27] A. P. Velmuzhov, M. V. Sukhanov, T. V. Kotereva, N. S. Zernova, V. S. Shiryaev, E. V. Karaksina, B. S. Stepanov, M. F. Churbanov, *J. Non. Cryst. Solids* **2019**, *517*, 70.

[28] K. F. Palmer, D. Williams, *J. Opt. Soc. Am.* **1974**, *64*, 1107.

[29] E. A. Romanova, S. Korsakova, M. Komanec, T. Nemecek, A. Velmuzhov, M. Sukhanov, V. S. Shiryaev, *IEEE J. Sel. Top. Quantum Electron.* **2017**, *23*, 289.

[30] S. Guo, S. Albin, *Opt. Express* **2003**, *11*, 215.

[31] A. M. Stolyarov, A. Gumennik, W. McDaniel, O. Shapira, B. Schell, F. Sorin, K. Kuriki, G. Benoit, A. Rose, J. D. Joannopoulos, Y. Fink, *Opt. Express* **2012**, *20*, 12407.

[32] A. Gumennik, A. M. Stolyarov, B. R. Schell, C. Hou, G. Lestoquoy, F. Sorin, W. McDaniel, A. Rose, J. D. Joannopoulos, Y. Fink, *Adv. Mater.* **2012**, *24*, 6005.

[33] A. Yildirim, M. Vural, M. Yaman, M. Bayindir, *Adv. Mater.* **2011**, *23*, 1263.

[34] M. Evrard, T. Combes, A. Maldonado, F. Désévédavy, G. Gadret, C. Strutynski, J. C. Jules, C. H. Brachais, F. Smektala, *Opt. Mater. Express* **2022**, *12*, 136.

[35] G. Tao, H. Ebendorff-Heidepriem, A. M. Stolyarov, S. Danto, J. V. Badding, Y. Fink, J. Ballato, A. F. Abouraddy, *Adv. Opt. Photonics* **2015**, *7*, 379.

[36] B. Zhang, W. Guo, Y. Yu, C. Zhai, S. Qi, A. Yang, L. Li, Z. Yang, R. Wang, D. Tang, G. Tao, B. Luther-Davies, *J. Am. Ceram. Soc.* **2015**, *98*, 1389.

[37] K. Wu, X. Song, S. Cui, Z. Li, Y. Jiao, C. Zhou, *Appl. Surf. Sci.* **2018**, *451*, 45.

Table of content

Evolutive fiber geometries featuring thin polymer structures are fabricated using the thermal-drawing process. A sandwich-like architecture is produced to assess the fiber-drawing ability of the proposed preform profiles. The fabrication methodology is applied to a more sophisticated geometry from which quasi-exposed-core waveguides can be produced. Evanescent-wave sensing experiments are carried out using the processable fiber structure.

Dr. C. Strutynski,* Dr. M. Deroh, R. Bizot, M. Evrard, Dr. F. Désévédavy, Dr. G. Gadret, Dr. J.-C. Jules, Dr. C.-H. Brachais, Dr. B. Kibler and Prof. F. Smektala

Evolutive optical fibers combining oxide and chalcogenide glasses with submicronic polymer structures

ToC figure